Resistivity and Carrier Mobility of the $SmBa_2Cu_3O_{6+x}$ Superconductor with Different Oxygen Doping Levels

G. Spinolo, P. Ghigna, G. Chiodelli, M. Ferretti[a], and G. Flor

Dipartimento di Chimica fisica, INSTM, and C.S.T.E./CNR Università di Pavia, Viale Taramelli 16, I-27100 Pavia
[a] Dipartimento di Chimica e Chimica Industriale and INFM, Università di Genova, Via Dodecaneso 31, I-14146 Genova

Z. Naturforsch. **54a**, 95–100 (1999); received December 21, 1998

DC conductivity measurements between 15 and 300 K are reported for $SmBa_2Cu_3O_{6+x}$ samples with different oxygen doping amounts (x) produced by annealing under appropriate high temperature and oxygen pressure conditions and quenching.

Samples with $x \geq 0.5$ are superconductors: $T_c \sim 60$ K at $x = 0.7$, $T_c > 80$ K at $x = 0.9$. The transition from superconduction to non-superconduction corresponds to the tetragonal to orthorhombic structural transition and to the transition from semiconducting to metallic temperature dependence of the resistivity.

Oxygen doping causes a sudden increase of hole mobility near $x = 0.5$. Below this threshold, the behavior of the carrier mobility is in agreement with an Anderson localization.

Introduction

This paper is part of an experimental investigation on the influence of *extrinsic* doping (i.e. doping due to oxygen non-stoichiometry) on the charge transport properties of oxide superconductors. When one dopes a material having the non-superconducting reference stoichiometry, only small changes in the amount and mobility of the charge carriers are initially produced. However, when a critical value of doping is reached, superconductivity arises quite suddenly, and the carrier mobility also shows sudden changes, which are different for different materials. In *n*-doped NCCO ($Nd_{2-x}Ce_xCuO_{4\pm\delta}$, $x \sim 0.15$) [1, 2], for instance, the effective mass of the electronic carriers increases and their mobility decreases when the amount of doping reaches the critical value. The carriers can be described here as large polarons: experimental evidence [2] indicates that the doping level corresponding to the onset of superconductivity also corresponds to the onset of a coupling between these carriers well above T_c.

An opposite trend occurs in *p*-doped BSCCO-2212 (the material usually written as $Bi_2Sr_2CaCu_2O_{8+\delta}$). When the carriers reach a critical density, their mobility shows here a sudden *increase* from ~ 0.1 to ~ 1 $cm^2 V^{-1} s^{-1}$ with only a small change of intrinsic doping [3]. In addition to the different sign of the carriers, a remarkable difference between NCCO and BSCCO materials is that the former family exhibits a single band at the Fermi level, whereas the electronic structure of the latter one is made more complex by the presence of a Bi-O band. This adds intrinsic doping to extrinsic doping, making possible an electron transfer between Cu-O and Bi-O layers, or an internal oxydation, in chemical words.

For the above purpose, the $REBa_2Cu_3O_{6+x}$ (RE = Y, or rare earth) family provides the most interesting field of research because of its possibility of introducing small changes of the underlying electronic structure using different RE cations. We here investigate the electrical conductivity between 10 and 300 K of $SmBa_2Cu_3O_{6+x}$ (hereafter denoted Sm-123) samples prepared with different oxygen contents and we discuss its behavior on the basis of previous conductivity and oxygen non-stoichiometry determinations at high-temperatures and under various oxygen pressures, where the solid phase is in equilibrium with external oxygen [4]. Papers in preparation will deal with the Nd and Eu members of the same family.

Experimental

Sm-123's were prepared by a sol-gel technique [4] starting from Sm_2O_3 (Aldrich, 99.9%), $BaCO_3$ (Fluka, >99.0%), and CuO (Fluka, 99%) to obtain citrate precursors. Stoichiometric amounts of them were then reacted in air at 900 °C for 20 hours, with a final sintering step at 940 °C for 20 further hours. The samples were always kept under oxygen pressures not exceeding 10^{-1} atm,

Reprint requests to Prof. Giorgio Spinolo; Fax: 0382-507575.

0932-0784 / 99 / 0200-0095 $ 06.00

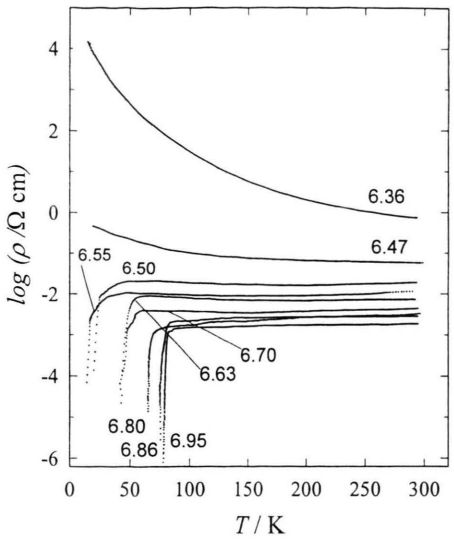

Fig. 1. Resistivity vs. T of $SmBa_2Cu_3O_{6+x}$ samples: the labels indicate the oxygen content.

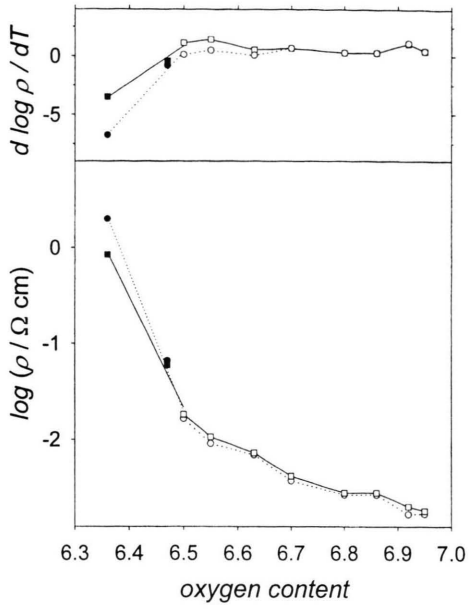

Fig. 2. Trend with oxygen content of the resistivity (lower part) and temperature derivative of the resistivity (upper part). Empty symbols: superconducting samples; filled symbols: non-superconducting samples. Squares: data for 200 K; circles: data for 273 K.

to avoid deviation from the 1 : 2 : 3 cation molecularity [4, 5].

After synthesis and sintering, different portions of the same batch were annealed under different [T, $P(O_2)$] conditions to unambiguously fix their oxygen content (x), and quenched. The [T, $P(O_2)$] conditions required to achieve a particular x value, and the time required to reach equilibrium with external oxygen, were obtained from our previous determination of the relationships between x, T, and $P(O_2)$ [4]. The temperatures of the annealing steps were always higher than 400 °C.

The electrical conductivity was measured with a four electrode setup using a Solartron 1286 instrument as both galvanostat and voltmeter [6]. The measurements were made in the 10÷300 K range using a Leybold ROK 10–300 cryogenerator and two additional temperature transducers placed on the lower and the upper surface of the pelletizated sample. A PC with IEEE 488 interface was used to obtain temperature and voltage readings under slow cooling condition, and to control the agreement of the two independent temperature readings.

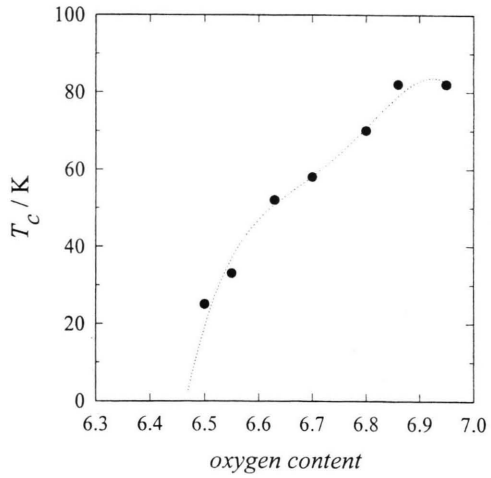

Fig. 3. Critical transition temperature for superconductivity as a function of oxygen content.

Results and Discussion

Figure 1 shows on a logarithmic scale the resistivity at and below room temperature of different samples with a given *oxygen content* [$6+x$ in $SmBa_2Cu_3O_{6+x}$], as obtained by quenching from appropriate [T, $P(O_2)$] conditions. The resistivities at 273 and 200 K are compared as a function of x on the lower part of Figure 2. For the same compositions, the superconducting critical transition temperatures are shown on Figure 3.

It is worth recalling here our previous *high temperature* conductivity measurements *under equilibrium con-*

ditions with external oxygen [4]. An increase of conductivity with increasing temperature under *constant oxygen pressure* was then observed at oxygen contents below ~0.20. In this x range and at high temperature, the carriers are electron-hole couples-produced by intrinsic ionization. At higher doping levels, however, the predominant carriers are holes coupled to charged point defects: their amount is controlled by the equilibrium with external oxygen and is therefore strongly related to the oxygen content. The conductivity measurements above room temperature have therefore proved the oxygen content as being the main thermodynamic variable to be changed in order to change the nature and amount of charge carriers, at least in the range of doping relevant to the superconductivity transition.

According to the present results (upper part of Fig. 2), samples undergoing transition to a superconduction state when cooled (hereafter: superconducting samples) are characterized by a (small) positive slope of the ρ vs. T plots near room temperature. The superconducting samples correspond to $x \geq 0.5$. On the contrary, non-superconducting samples correspond to a (larger) negative slope of the ρ vs. T plots near room temperature. In the resistivity vs. x plots (lower part of the same figure), the onset of superconductivity is also indicated by a drift from linearity (on the logarithmic scale) at a resistivity value in the range of ten mΩ cm. For superconducting samples, ρ (273 K) and ρ (270 K) do not change by more than one order of magnitude and show a wavelike trend as x increases. There is here a marked similarity with the Y member [7], where the oscillation is much more marked and produces a real maximum.

The T_c vs. x trend (Fig. 3) agrees with that already reported in the literature for this compound [8] and is consistent with the trend shown by other $REBa_2Cu_3O_{6+x}$ compounds (see [7], [9], [10], and [11]). Starting from the low x side, here we see a first sudden increase to $T_c \sim 60$ K, then another jump to a plateau where the maximum T_c is reached. An intermediate plateau near $T_c = 60$ K is hardly seen here but is well apparent in the Dy, Yb, and Y members of the family: the first jump here occurs at a higher x value than in the Y compound, but at a lower x than in the Nd compound. The second jump, at $x \sim 0.8$, is not very different for the three compounds. This behavior agrees with the reported decrease of the T_c plateaus with the increase of the RE ionic radius [12].

The $x \sim 0.5$ value corresponding to the boundary between non-superconducting and superconducting samples roughly corresponds also to the boundary between tetragonal (at low x) and orthorhombic structure (at high x).

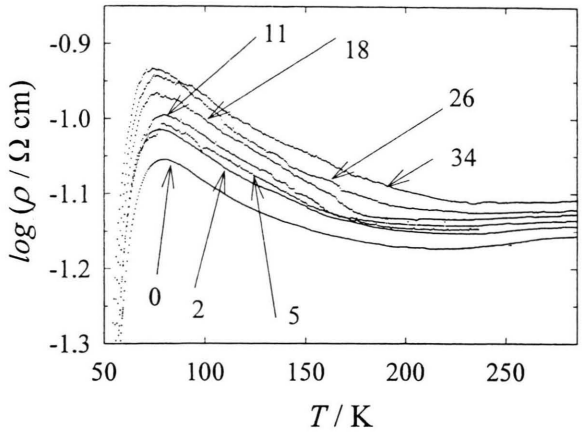

Fig. 4. Resistivity vs. T of an $SmBa_2Cu_3O_{6+x}$ sample after quenching (label "0") and after 2, 5, ... , 34 days storage at room temperature.

Actually, we must quote four similar x values for the properties of $SmBa_2Cu_3O_{6+x}$: a) the onset of superconductivity at $0.47 < x < 0.50$ (Fig. 3); b) the change of sign of the slope $d\rho/dT$ near and above room temperature, which also occurs at $0.47 < x < 0.50$ (Fig. 2); c) the change of the slope of the σ vs. x curves at high temperatures, as already said [4]; and d) the change of the powder X-ray patterns [4]. The latter two occur at $x \sim 0.55$.

In comparing these similar x values, additional phenomena, such as the ordering of oxygen vacancies and the appearance of the so called orthorhombic II phase must be considered. For instance, Fig. 4 reports $\log \rho$ vs. x data for a single sample with $x = 0.5$ immediately after quenching (data labelled with "0"), and stored for 2, 5, 11, 18, 26, and 34 days at room temperature. A decrease of conductivity and of T_c are well apparent in the very enlarged scale of the ρ axis, and show that some reordering of the point defects quenched from high temperature occurs also at room temperature. The influence of these phenomena on the appearance of superconductivity in these materials is a debated problem in current literature (see [9], [11–17]). For what concerns the present work, we note here that the fine scale of the resistivity changes reported on Fig. 4 shows the effectiveness of the quenching procedure in preparing samples with a fixed oxygen content. The ordering of oxygen-related point defects also offers a reasonable explanation for the above slight discrepancies concerning the boundary x value between superconducting and non-superconducting materials.

The hole injection sequence has been discussed by several Authors, for instance by [7], [18–20]. We here refer

to the experimental investigation by Tolentino et al. [18] on Y-123 and on its quite complex results. With a strong simplification, the hole injection sequence can be described as follows:

a) starting from the $x=0$ stoichiometry and up to $x\sim 0.2$ (in $YBa_2Cu_3O_{6+x}$), extrinsic doping produces strongly localized holes on Cu (I) sites. These can also be seen as positively charged Cu (II) point defects: $Cu^{\cdot}_{Cu\,(I)}$.
b) At higher doping levels and up to the tetragonal/orthorhombic phase transition, each additional oxygen atom produces one hole with predominant O-2$p_{x,y}$ character. These holes are localized on the Cu-O chains along the c axis of the crystal structure.
c) With doping levels above the structural phase transition, the newly injected holes still have predominant O-2$p_{x,y}$ character and are produced at a rate of 1 hole/l doping oxygen, but are localized on the CuO_2 planes. These are the most mobile holes.
d) At the highest doping levels, also holes with predominant O-2p_z must be considered.

Now, we want to show that it is possible to gain some understanding of the transport properties of $SmBa_2Cu_3O_{6+x}$ making reference to this schematic injection sequence of $YBa_2Cu_3O_{6+x}$. For that purpose, it is convenient to consider a simplified model where:

i) holes of kinds a) and d) are not taken into account,
ii) the overall conductivity is written as the sum of independent contributions from holes of kinds b) and c):

$$\sigma_{tot}=\sigma_b+\sigma_c,$$

iii) each contribution is in turn written as the product of a hole concentration p times a *constant* hole mobility μ:

$$\sigma_i=q\cdot\mu_i\cdot p_i,$$

where q is the elementary charge,
iv) the amount of holes of kind b) changes linearly with doping with slope = 1 (on a molar scale) between $x=0.2$ and $x=0.5$ (where the tetragonal/orthorhombic transition takes place in $SmBa_2Cu_3O_{6+x}$) but is otherwise constant to zero ($x<0.2$) or 0.3 ($x>0.5$), and finally,
v) the amount of holes of kind c) changes linearly with doping with slope = 1 above $x=0.5$.

The results of this simplified analysis are displayed on Figure 5. They show that the tetragonal/orthorhombic structural transition corresponds to a marked change (from $\sim 10^{-2}$ to $\sim 10^{0}$ $cm^2\,V^{-1}\,s^{-1}$) of the mobility of the carriers both at room temperature and at 200 K. We also note that above the superconductivity transition, the mobility of the charge carriers does practically not change with the amount of doping, and that the mobility values above $x=0.5$ are typically those of large polarons, in agreement with our previous findings [4].

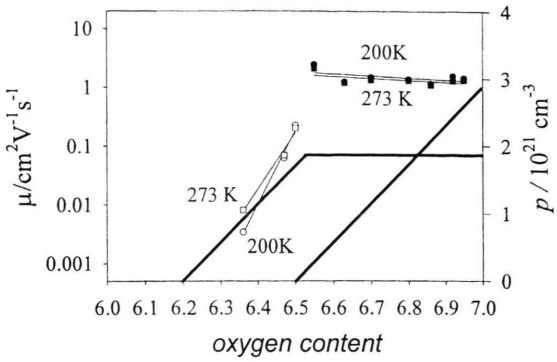

Fig. 5. Mobility of the predominant carriers as a function of oxygen content. Empty symbols: non-superconducting samples; filled symbols: superconducting samples. Squares: data for 273 K; circles: data for 200 K. The heavy lines and the right scale indicate the underlying (simplified) model for hole injection. The right scale shows a number density (holes per unit volume).

Let us now discuss the non-superconducting samples. The ρ (273 K) and ρ (200 K) values of these samples are higher than those of the superconducting samples, and are also higher than their high temperatures counterparts. Moreover, the resistivity differences are the higher the lower is x. These samples show around room temperature an activated conductivity, and the conductivity increases with oxygen content: extrinsic doping produces positive carriers.

The combined T-x dependence of the conductivity of these carriers can be related to two models.

On one hand we have the small polaron model [21] which essentially describes the response of largely non-interacting defects with almost the same features. In this case, we expect for σ

$$\sigma=p\,q\,\mu=p\,q\,\mu_0\exp(-E_a/kT),$$

where q is the elementary charge, p is the amount of carriers, μ is their mobility, and the parameters μ_0 and E_a are independent (or almost independent) of x.

On the other side we have various situations referred to as Fermi-level fluctuations and Anderson localization. Let us discuss the subject within the framework of the latter model. In the Anderson localization model, the electronic structure of a solid with a large amount

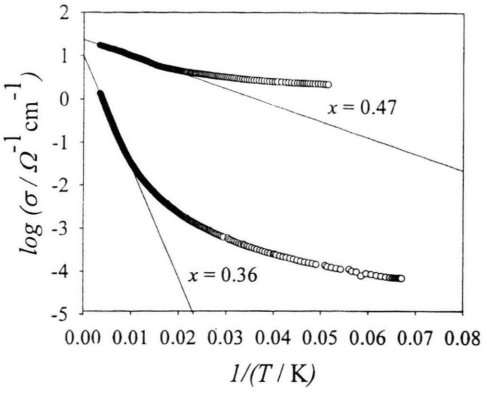

Fig. 6. Arrhenius plots for two non-superconducting samples of $SmBa_2Cu_3O_{6+x}$.

of similar and interacting defects is described starting from an energy distribution of localized electronic states. States lying well inside the energy range are strongly coupled to each other giving rise to delocalized states, while states lying on the tails of the energy distribution remain localized because fewer nearby interacting states are available. As a result, when the number of carriers is very low (or very high), i.e. the whole energy range is almost empty (or almost filled), the carriers enter strongly localized states and are therefore characterized by a low mobility with a temperature dependence controlled by an activation energy. Instead, when the whole energy range is close to be half-filled, the carriers at the Fermi level have a much larger mobility which decreases with temperature (because of scattering). For this model we expect a smooth transition between an activated and a metallic-like conductivity when the amount of defects (i.e. the amount of extra oxygens) is increased. In particular, we expect a) for the small polaron model: σ vs. T trends in close agreement with an Arrhenius law and an activation energy that does not depend significantly on the doping level, and b) for the Anderson localization model: σ vs. T trends different from an Arrhenius law and "apparent" activation energies going from high values (with low amount of doping) to zero (when the doping is "large enough"). Figure 6 shows that for both reasons the latter one is indeed the most suitable model for reduced ($x<0.5$) $SmBa_2Cu_3O_{6+x}$.

Conclusions

The resistivity of $SmBa_2Cu_3O_{6+x}$ strongly changes with the oxygen doping amount (x). Below $x\sim0.5$, the materials do not show a superconducting transition, belong to the tetragonal structure, and are characterized by a (large) negative derivative of resistivity with respect to temperature. Above this threshold, the materials become superconductors at low temperature, belong to the orthorhombic structure, and are characterized by much lower resistivities and by a (smaller) positive derivative of resistivity with respect to temperature.

The trend of T_c with x is analogous to that shown by the Y and other RE-123 oxide superconductors and shows an intermediate plateau near $T_c=60$ K.

Using an approximate hole injection sequence derived from literature data for Y-123, it is possible to show that the oxygen doping corresponding to the superconductivity onset also corresponds to a sudden change of hole mobility.

In the semiconducting range, the mobility of carriers is better in agreement with an Anderson localization than with a small polaron model.

Acknowledgement

This work has been partially supported by the Department of University and Scientific and Technological Research of the Italian Government (MURST-Programmi nazionali di ricerca).

[1] P. Ghigna, G. Spinolo, M. Scavini, G. Chiodelli, G. Flor, and A. V. Chadwick, Physica C **268,** 150 (1996).
[2] M. Scavini, P. Ghigna, G. Spinolo, U. Anselmi-Tamburini, G. Chiodelli, G. Flor, A. Lascialfari, and S. De Gennaro, Phys. Rev. B **58,** 9385 (1998).
[3] Work in preparation by the present Authors (1998).
[4] G. Chiodelli, I. Wenneker, P. Ghigna, G. Spinolo, G. Flor, M. Ferretti, and E. Magnone, Physica C **308,** 257 (1998).
[5] L. Dimesso, O. B. Hyan, and I. Mirabayashi, Physica C **248,** 127 (1995).
[6] G. Chiodelli, G. Campari-Vigano, and G. Flor, Z. Naturforsch. **44a,** 1167 (1989).
[7] R. J. Cava, B. Batlogg, C. H. Chen, E. A. Rietman, S. M. Zahurak, and D. Werder, Phys. Rev. B **36,** 5719 (1987).
[8] M. Buchgeister, W. Hiller, S. M. Hosseini, K. Kopitzki, and D. Wagener, in Proc. Int. Conf. Transport Properties of Superconductors, Rio de Janeiro, R. Nicolsky ed., World Scientific, Singapore 1990, p. 511.
[9] S. Libbrecht, E. Osquiguil, B. Wuyts, Z. X. Gao, and Y. Bruynseraede, Physica C **206,** 512 (1993).

[10] H. Ishizuka, Y. Idemoto, and K. Fueki, Physica C **195,** 145 (1992).
[11] A. Krekels, V. Zou, G. Van Tendeloo, D. Wagener, M. Buchgeister, S. M. Hosseini, and P. Herzog, Physica C **196,** 363 (1992).
[12] M. Buchgeister, S. M. Hosseini, K. Kopitzki, and D. Wagener, in High Temperature Superconductors – Physics and Materials Science, NATO ASI Series E 181 (1990), p. 319.
[13] B. W. Veal, H. You, A. P. Paulakis, H. Shi, Y. Fang, and J. W. Downey, Phys. Rev. B **42,** 4770 (1990).
[14] E. Straube, D. Hohlwein, and F. Kubanek, Physica C **295,** 1 (1998).
[15] V. E. Zubkus, O. E. Parfionov, E. E. Tornau, and P. J. Kundrotas, Physica C **198,** 141 (1992).
[16] G. V. Uimin, V. F. Gantmakher, A. M. Neminsky, L. A. Novomlinsky, D. V. Shovkun, and P. Brüll, Physica C **192,** 481 (1992).
[17] V. Zou, A. Krekels, G. Van Tendeloo, D. Wagener, M. Buchgeister, S. M. Hosseini, and K. Kopitzki, in Atomic Structures of High-T_c Superconductors, K. H. Kuo and J. P. Zhang Eds., Trans. Tech. Publications, Aedermannsdorf, Switzerland 1993, p. 41.
[18] H. Tolentino, F. Baudelet, A. Fontaine, T. Gourieux, G. Krill, J. Y. Henry, and J. Rossat-Mignod, Physica C **192,** 115 (1992).
[19] A. R. Moodenbaugh and D. A. Fischer, Physica C **230,** 177 (1994).
[20] K. Widder, D. Berner, H. P. Geserich, W. Widder, and H. F. Braun, Physica C **251,** 274 (1995).
[21] J. Tateno, Physica C **214,** 337 (1993).